https://doi.org/10.5194/gmd-2022-177
Preprint. Discussion started: 22 August 2022

Geoscientific Model Development Discussions

ForamEcoGENIE 2.0: Incorporating symbiosis and spine traits into a trait-based global planktic foraminifera model

Rui Ying[1], Fanny M. Monteiro[2], Jamie D. Wilson[1], Daniela N. Schmidt[1]

[1]School of Earth Sciences, University of Bristol, Bristol, BS8 1RJ, UK
[2]School of Geographical Sciences, University of Bristol, Bristol, BS8 1SS, UK

Correspondence to: Rui Ying (rui.ying@bristol.com)

Abstract. Planktic foraminifera are major marine calcifiers in the modern ocean regulating the marine inorganic carbon pump and generating marine fossil archives of past climate change. Some planktic foraminifera evolved spine and symbiosis, increasing functional trait diversity and expanded their ecological niches. Here we incorporate symbiosis and spine traits into the ForamEcoGENIE model, a trait-based model focusing on functional trait rather than individual species, to enable us to study the importance of foraminifera biodiversity in the palaeoceanographic environment. We calibrated the modelled new traits using Latin Hypercube Sampling. We identified the best model run from an ensemble of 1200 runs compared with observations from global core-top, sediment trap, and plankton nets. The model successfully captures the global distribution and seasonal variation of the 4 major functional groups including dominance of the symbiont-obligate type in subtropical gyres and the symbiont-barren type in the productive subpolar oceans. The carbon export rate is correctly predicted for spinose foraminifera, but the model overestimates the global mean biomass of each group by 8 times and global export rate of non-spinose foraminifera by 4 times. Both the observational bias and the model's limitation in linking biomass to export production likely contributes to the discrepancy. Our model approximates a 3.05 g m^{-2} yr^{-1} global mean foraminifer-derived calcite flux and 1.1 Gt yr^{-1} total calcite export, account for 19% of the global pelagic marine calcite budget within the lower range of modern calcite estimates. The calcite export is mostly derived from the symbiont-barren non-spinose group (39%) and the symbiont-obligate spinose group (13%). Our model overcomes the lack of biodiversity in previous version and offers the potential to explore foraminifera ecology dynamics and its impact on biogeochemistry in modern, future and paleogeographic environments.

https://doi.org/10.5194/gmd-2022-177
Preprint. Discussion started: 22 August 2022

Geoscientific Model Development Discussions

1 Introduction

Planktic foraminifera are marine calcifying zooplankton that have populated the surface ocean since the mid-Jurassic (~175 Ma). They produce calcite shells, preserved in vast amounts in sediments, that provide proxy archives (e.g., ^{13}C, ^{18}O, Mg/Ca) to reconstruct past climate conditions (Tierney et al., 2020), ocean carbonate chemistry (Hönisch et al., 2012) and study biotic response to environmental change (Todd et al., 2020). In the modern oceans, foraminifera contribute 23-56% of the total open-ocean $CaCO_3$ export (Schiebel, 2002) alongside the other major calcifiers, coccolithophores (Daniels et al., 2018) and pteropods (Buitenhuis et al., 2019). However, understanding the impacts of environmental change on foraminifers and their role in the carbon cycle is challenged by their low standing stocks in the surface ocean, a (semi)lunar reproductive cycle driving abundances and difficulties in culturing to ground truth physiology (Schiebel and Hemleben, 2017). Modelling planktic foraminifera and their ecology, therefore, plays a critical role in increasing and testing our understanding of their biological and ecological influence on the marine inorganic carbon cycle and their role as a paleo-proxy carrier.

The recent decades have seen significant developments of global foraminifera models due to the increasing data compilations of foraminifer flux and community structure (Siccha and Kucera, 2017; Buitenhuis et al., 2013; Sunagawa et al., 2020). Žarić et al. (2006) constructed the first global-scale prediction on foraminifer flux using a statistical technique that correlated hydrographical factors and sediment trap abundance of 18 main species. Fraile et al. (2008) and Lombard et al. (2011) built an ecophysiology based dynamic model PLAFOM and FORAMCLIM based on CESM (Hurrell et al., 2013) and PISCES (Aumont et al., 2015), respectively. These two models reconstructed seasonal production in Last Glacial Maximum (LGM) (Fraile et al., 2009), vertical distribution dynamics (Kretschmer et al., 2018) and potential diversity change in response to projected high-emission scenarios (Roy et al., 2015). However, the species-based feature of these models causes limitations for applications. For example, parameterisation limits the inclusion of additional species, which are less well understood ecologically. Moreover, while these models are applied to LGM and future oceans, the application to deeper time is severely limited by the existence of extinct species and cryptic taxa with novel ecologies (Renaud and Schmidt, 2003) and non-analogue situations, i.e., time intervals older than the Miocene with many none extant species, cannot be assessed with confidence.

Trait-based models of plankton ecology can overcome the challenges of species-based models. This approach focuses on organismal traits including morphological and physiological properties instead of taxonomic identities to reduce model complexity, capture ecological interaction (Zakharova et al., 2019) and identify drivers of community assembly under global changes (Enquist et al., 2015). Models adopting trait-based framework have successfully resembled the diverse marine community such as cyanobacteria (Follows et al., 2007) and diazotroph (Monteiro et al., 2010), usually by defining physiological characteristics and relevant trade-offs (e.g., size-class of plankton). Undoubtedly, this strategy provides a simple but mechanistic way to mimic the complex real ocean ecology (Kiørboe et al., 2018).

https://doi.org/10.5194/gmd-2022-177
Preprint. Discussion started: 22 August 2022


Geoscientific Model Development Discussions

Understanding of foraminifer traits and their functions is crucial for developing a trait-based model. The foremost trait of foraminifer is calcification, with foraminifera building a shell by adding calcite chambers during their development (Caromel et al., 2015). In addition, 19 out of ~50 modern foraminifer species bear eukaryotic algae such as dinoflagellates, chrysophytes and haptophyte as symbionts (Takagi et al., 2019). Spines and symbiosis are crucial functional traits of planktic foraminifers and dividing the group in their phylogeny study (Morard et al., 2018). Symbionts assimilate nutrients, which can be translocated to the host, providing extra energy in the nutrient-deficient environment to the foraminifer (LeKieffre et al., 2018; Ortiz et al., 1995; Uhle et al., 1999). Core-top data (Siccha and Kucera, 2017) show that species with symbionts are mainly found in the low latitudes and open oceans, while non-symbiotic foraminifers dominate the temperate to polar regions (Figure 1). Furthermore, symbiont-obligate foraminifers that cannot live without their symbionts prefer the low latitude to the symbiont-facultative group which can flexibly bear symbionts and have a wider geography (Figure 1). Another important trait is spines extruding from the test, present in roughly half of modern species. These spinose species are mostly symbiotic (except symbiont-barren *Globigerina bulloides* and *Hastigerina pelagica)* and show a preference for omnivorous feeding (Schiebel and Hemleben, 2017). Therefore, traits affect biogeography and trophic activities and lay the foundation of building a trait-based model.

Recently, Grigoratou et al., (2019) developed the first trait-based model for non-spinose foraminifer and coupled it to cGENIE (ForamEcoGENIE, Grigoratou et al., 2021a), an Earth System Model of intermediate complexity allowing for fast computational time and widely applied to past climates: Palaeocene–Eocene Thermal Maximum (Ridgwell and Schmidt, 2010), Last Glacial Maximum (Rae et al., 2020) and Cretaceous-Paleogene boundary (Henehan et al., 2019). Such computational efficiency and abundant applications make ForamEcoGENIE easily applicable to a wide range of geological periods with direct links with seawater carbon chemistry and isotope tracers. In this study, we extend ForamEcoGENIE to resolve 3 more critical functional groups of planktic foraminifera by adding the traits of symbiosis and spines (tested in Grigoratou et al., 2021b). Thereby, we build a model that can explore foraminifer ecogroups in past climates (Ezard et al., 2011). We compare the model with three global observational data compilations (core-top, plankton net tow and sediment traps) and test its ability to produce surface biomass, organic carbon and calcite flux rate, and relative abundance distribution.

https://doi.org/10.5194/gmd-2022-177
Preprint. Discussion started: 22 August 2022

Geoscientific Model Development Discussions
Open Access
EGU

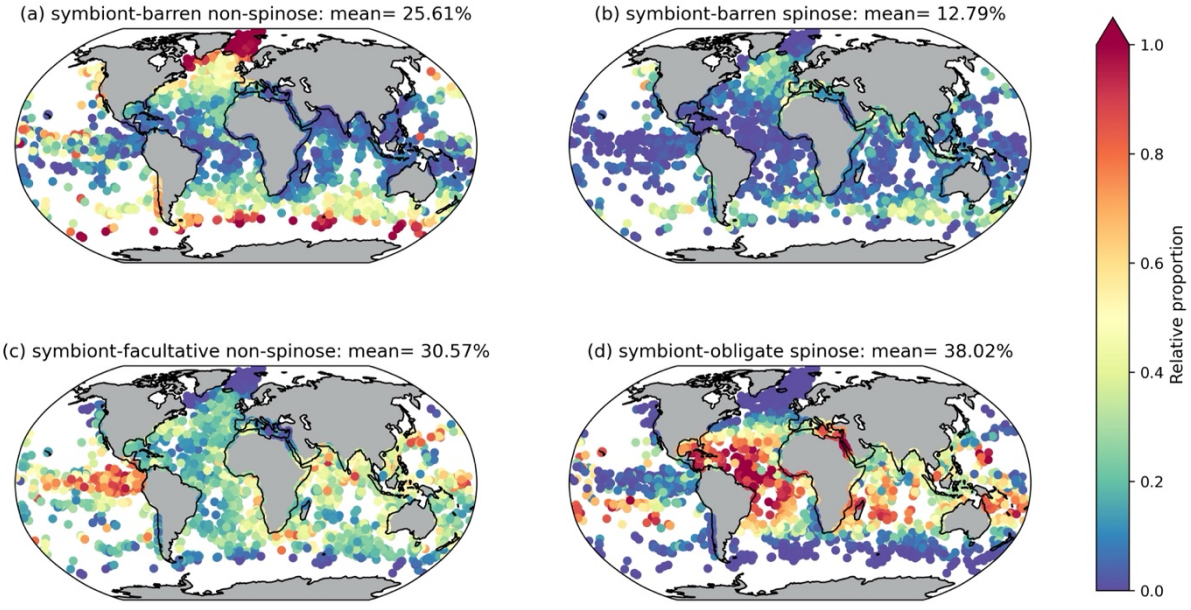

Figure 1: Relative proportion in shell abundance of planktic foraminifer functional groups. Data source: ForCenS core-top dataset (Siccha and Kucera, 2017).

2 Model description

2.1 Ocean and atmosphere physics

ForamEcoGENIE uses cGENIE (carbon-centric Grid-ENabled Integrated Earth system model), a modular Earth system model of intermediate complexity (EMIC) as the physical ocean simulation framework. The fast climate and ocean physics of cGENIE are based on a coarse-resolution 3D frictional geostrophic ocean model coupled to a 2D energy-moisture-balance atmosphere model and a dynamic-thermodynamic sea-ice model (Edwards and Marsh, 2005; Marsh et al., 2011). The ocean has a 36x36 equal-area horizontal grid (uniform in longitude and sine-uniform in latitude) with 16 logarithmically spaced vertical levels as defined in Cao et al., (2009). The physical model is coupled with a model of ocean biogeochemical cycles (Ridgwell et al., 2007; van de Velde et al., 2021), and sea-floor sedimentary processes (Ridgwell and Hargreaves, 2007) and marine ecosystem processes (Ward et al., 2018). The plankton ecosystem is resolved in the surface layer (0-80.8 m) to mimic light limitation. The model presented in this study is configured with a seasonally forced pre-industrial climate state and a fixed atmospheric CO_2 concentration restored to 278 ppm.

https://doi.org/10.5194/gmd-2022-177
Preprint. Discussion started: 22 August 2022


Geoscientific Model Development Discussions

2.2 Allometric and trait-based plankton ecosystem framework

We employ the trait-based marine plankton ecosystem model EcoGENIE (Ward et al., 2018) to simulate foraminifera's physiological processes and ecological interactions with other plankton. In this section, we summarise the core concepts specific to foraminifera modelling and refer the readers to Ward et al. (2018) for the full description of the model.

In EcoGENIE, individual body size determines key physiological processes, including nutrient uptake, photosynthesis, grazing gain and predation through allometric scaling (West et al., 1997), because of its role as a master trait among pelagic organisms (Andersen et al., 2016). The modelled size-dependent parameters (except for photosynthesis) follow a generic power law: $P = aV^b$ with P the size-based parameter, V the spheric biovolume, and a, and b the allometric intercept and exponent.

A fundamental size-based concept is the plankton cell quota. The plankton size (biovolume, V) determines the carbon quota content (Q_C) following a power law (with scaling coefficient and exponent b, Equation 1). The ratio of other assimilated nutrients (B_{i_b}, i_b stands for the i^{th} population nutrient biomass: P, Fe, or chlorophyll) to carbon biomass (B_C) represents the plankton group's physiological status with dynamic stoichiometry ($\mathrm{Q_{i_b}}$, Eqn. 2) (Droop, 1968; Flynn, 2008). Based on this cell quota status, the limitation term for each nutrient ($Q_{i_b}^{\mathrm{stat}}$) is formulated as per Geider et al., (1998), where nutrient uptake rate gradually slows down when the internal inorganic nutrient quota is close to its maximum value ($\mathrm{Q_{i_b}^{max}}$, Eqn. 3). The nutrient quota range ($\mathrm{Q_{i_b}^{min}}$, $\mathrm{Q_{i_b}^{max}}$) is proportional to the carbon quota (Q_C).

$$Q_C = \mathrm{aV}^b \tag{1}$$

$$Q_{i_b} = \frac{B_{i_b}}{B_C}, \qquad i_b = P, Fe, Chl \tag{2}$$

$$Q_{i_b}^{\mathrm{stat}} = \left(\frac{\mathrm{Q_{i_b}^{max}} - \mathrm{Q_{i_b}}}{\mathrm{Q_{i_b}^{max}} - \mathrm{Q_{i_b}^{min}}}\right)^{0.1} \tag{3}$$

Metabolic processes in EcoGENIE are temperature dependent, as in the universal metabolic theory (Brown et al., 2004). Ectothermic plankton's body temperature is determined by the ambient seawater environment (T). Temperature regulation γ_T acts on metabolic processes including respiration, nutrient uptake, and predation and is modelled through an Arrhenius-like function (Eqn. 4), where the parameter A determines temperature sensitivity and reference temperature (T_{ref}) is the temperature allowing $\gamma_T = 1$.

$$\gamma_T = e^{A(T - T_{\mathrm{ref}})} \tag{4}$$

The biomass of any plankton group (j) and element (i_b), $\mathrm{B_{j,i_b}}$, varies due to a combination of potential physiological processes that are determined by the type of organism: nutrient uptake, grazing gains, grazing losses, mortality, and respiration losses (Eqn. 5).

https://doi.org/10.5194/gmd-2022-177
Preprint. Discussion started: 22 August 2022

Geoscientific Model Development Discussions

$$\frac{\partial B_{j,i_b}}{\partial t} = \underbrace{V_{j,i_b} \cdot B_{j,C}}_{nutrient\ uptake} + \underbrace{B_{j,C} \cdot \lambda_{i_b} \sum_{j_{prey}=1}^{J} G_{j,j_{prey},i_b}}_{grazing\ gains}$$
$$\underbrace{- B_{j_{pred},C} \cdot \sum_{j_{pred}=1}^{J} G_{j_{pred},j,i_b}}_{grazing\ losses} - \underbrace{m_j \cdot B_{j,i_b}}_{mortality\ loss} - \underbrace{r_{j,C} \cdot B_{j,i_b}}_{respiration\ loss} \quad (5)$$

The inorganic resource state variables (R_{i_r}) varies with nutrient uptake (V_{j,i_r}) and DIC with the living organisms' respiration ($r_{j,C}$).

$$\frac{\partial R_{i_r}}{\partial t} = \begin{cases} \sum_{j=1}^{J} -V_{j,i_r} \cdot B_{j,C}, & i_r = Fe, P \\ \sum_{j=1}^{J} -V_{j,i_r} \cdot B_{j,C} + \sum_{j=1}^{J} r_{j,C}, & i_r = C \end{cases} \quad (6)$$

Additional sources and sinks of nutrients such as remineralisation of organic matter and air-sea gas exchange are computed in the biogeochemical module BIOGEM (Ridgwell et al., 2007).

2.3 ForamEcoGENIE 1.0 description

ForamEcoGENIE 1.0 accounted for two foraminifera traits, including the feeding behaviour and calcification (Grigoratou et al., 2019, 2021a). It implemented a predator-prey interaction ($G_{j_{pred},j_{prey}}$, Eqn. 7) using a Holling type II model (Holling, 1965), where the overall grazing rate depends on the total available prey ($F_{j_{pred}}$), the maximum grazing rate of predators (G^m_{pred}) and the half-saturation concentration of available food ($k_{j_{prey}}$), and is regulated by temperature limitation (γ_T), a prey-switching term (Φ), and a prey refuge protection ($1 - e^{\Lambda F_{j_{pred}}}$). The calcification trait was included by reducing foraminifera palatability (P_p which influences $F_{j_{pred}}$, Eqn. 8) and mortality rate (m_j, Eqn. 5) to account for higher protection against predators and infections to the expense of a lower G^m_{foram} (Eqn. 7).

$$G_{j_{pred},j_{prey}} = \underbrace{\gamma_T \cdot \lambda_h}_{\text{limitations}} \cdot \underbrace{\frac{G^m_{pred} F_{j_{pred}}}{\epsilon k_{j_{prey}} + F_{j_{pred}}}}_{\text{overall grazing rate}} \cdot \underbrace{\Phi_{j_{pred},j_{prey}}}_{\text{Switching}} \cdot \underbrace{\left(1 - e^{\Lambda F_{j_{pred}}}\right)}_{\text{prey refuge}} \quad (7)$$

$$F_{j_{pred}} = P_p \cdot B_{j_{prey}} \cdot \exp\left[-ln\left(\frac{\mu_{j_{pred},j_{prey}}}{\mu_{opt}}\right)^2 / 2\sigma^2_{j_{pred}}\right] \quad (8)$$

In the model, the predators select their preys (Eqn. 8) based on the predator-prey size ratio $\mu_{j_{pred},j_{prey}}$ relative to the optimal value μ_{opt}, predators' food range $\sigma^2_{j_{pred}}$, and the calcification protection P_p. The foraminifera in ForamEcoGENIE 1.0 were set as herbivores. Additional foraminifera traits defined by a spine effect (ϵ) and a mixotrophy cost (λ_h) are introduced in ForamEcoGENIE 2.0 (see section 2.4)

https://doi.org/10.5194/gmd-2022-177
Preprint. Discussion started: 22 August 2022


Geoscientific Model Development Discussions

The prey-switching term ($\Phi_{j_{\text{pred}},j_{\text{prey}}}$) simulates the feeding habitat of zooplankton (Eqn. 7). The exponential *s* defines the active level of zooplankton predators, which capture abundant prey with higher priority when *s* increases. All foraminifera are assumed to be ambush passive predators with s=1.

$$\Phi_{j_{\text{pred}},j_{\text{prey}}} = \frac{\left(F_{j_{\text{pred}}}\right)^s}{\sum_{j_{\text{prey}}=1}^{J}\left(F_{j_{\text{pred}}}\right)^s} \quad (9)$$

Finally, to further approach the reality, the refuge term ($1 - e^{\Lambda F_{j_{\text{pred}}}}$) in the Eqn. (7) is added to decrease grazing rate when prey availability lowers with the protection strength of Λ.

2.4 ForamEcoGENIE 2.0: improved calcification and more functional groups

Here, we expand ForamEcoGENIE 1.0 by adding symbiosis and spine traits to the foraminifera group to distinguish four functional groups of planktic foraminifera (Table 1). We also implement a new calcification trade-off relating calcification energetic cost to the respiration term.

Table 1. The four modelled functional groups of planktic foraminifera and their species representative in ForamEcoGENIE 2.0.

Spine trait	Symbiosis trait	Species example	Species number*	Model implementation
Spinose	Symbiont-obligate	*Globigerinoides ruber*	17	This study
Spinose	Symbiont-barren	*Globigerina bulloides*	*2*	This study
Non-spinose	Symbiont-facultative	*Neogloboquadrina dutertrei*	*5*	This study
Non-spinose	Symbiont-barren	*Neogloboquadrina pachyderma*	23	extended from ForamEcoGENIE 1.0

* Count from Schiebel and Hemleben, (2017)

2.4.1 Respiration cost

We modified the metabolic cost of calcification defined in Grigoratou et al. (2019, 2021a) by replacing the original reduced maximum growth rate (or specifically maximum grazing rate) with a temperature-dependent respiration loss term. We choose this new loss term over a reduced growth rate because (1) extra respiration is a more biologically realistic cost and (2) a temperature-dependent term helps reduce the low-latitude biomass as observed.

Metabolic cost

https://doi.org/10.5194/gmd-2022-177
Preprint. Discussion started: 22 August 2022


Geoscientific Model Development Discussions

The respiration r_j present in Eqn. 5 scales with carbon biomass and is multiplied by constant r_b and temperature limitation (Eqn. 10). We assumed that the lost carbon from respiration is instantly recycled back to DIC pool.

$$r_j = r_b \cdot \gamma_T \tag{10}$$

a. Mortality protection

The mortality loss term in the generic zooplankton scales with a basal rate constant m_b (Eqn. 5). Like in Grigoratou et al. (2019, 2021a), m_b for foraminifera is downscaled by a protection term P_m where a lower value of m_j indicates a higher protection from the foraminifera test against viral and bacterial infections.

$$m_j = P_m \cdot m_b \tag{11}$$

b. Protection from predators (palatability)

Like in ForamEcoGENIE 1.0, calcification protects from grazing and is defined by P_p, which reduces the biomass loss from predation (Eqn. 8).

2.4.2 Spine trait

Spines are foraminifer's taxonomical basis and are made up of calcite. The biological functions of spines are related to stability in water columns, symbiosis and feeding behaviour (Schiebel and Hemleben, 2017). The link with symbiosis is discussed separately in the following section.

a. Higher metabolic cost and reduced palatability

We assume that the metabolic cost and protection from the spines are characterised the same way as for calcification (Eqn. 10-11), with spinose foraminifera having a higher cost and a stronger protection than non-spinoses (Table 2).

b. Enhanced grazing

Studies show that spinose foraminifera are more efficient in capturing and digesting prey thanks to the spine and rhizopodia networks (Anderson and Bé, 1976). Spines widen the prey availability of immotile foraminifer and facilitate capturing larger preys, while non-spinose species cannot hold active prey and only accept smaller particles of copepods in the laboratory observations (Anderson et al., 1979; Hemleben et al., 1989). Grigoratou et al., (2021b) modelled such benefit by reducing the half-saturation constant (conventionally noted as $\boldsymbol{k}$ in a Michaelis-Menten model). Here we adopt this approach by reducing $k_{j_{\text{prey}}}$ by a scaling parameter ϵ ($0 < \epsilon < 1$; Eqn. 7).

2.4.3 Symbiosis trait

Symbiosis is a novel trait in the model, commonly seen in marine organisms including foraminifer. Many planktic foraminifera harbour algae (e.g., dinoflagellate, diatom) within their cell (Takagi et al., 2019). We represent these symbiotic species in the

https://doi.org/10.5194/gmd-2022-177
Preprint. Discussion started: 22 August 2022


Geoscientific Model Development Discussions

model as a single organism, which combines hetero- and autotrophy, equivalent to a calcifying mixotroph. We use the trait-based representation of mixotrophy of Ward and Follows, (2016), where any plankton can "naturally" predate and photosynthesize, where the alternative strategy for specialist group is turned off (i.e., V_m is 0 for zooplankton and G_m is 0 for phytoplankton), and for mixotrophs turned on. The cost of mixotrophy is that both autotrophy and heterotrophy parts (i.e., photosynthesis and grazing rates) are scaled down (by multiplying factor λ_s and λ_h with respect to symbionts and hosts, $0 < \lambda_s, \lambda_h < 1$) compared to the pure auto/heterotroph specialist (Ward and Follows, 2016). We also distinguish between symbiont-obligate and symbiont-facultative foraminifera using different λ_s/λ_h parameter values to reflect their different extent of dependency on symbionts (Table 2).

a. Symbiont cell size

We determine the cell size of the symbiont from a defined symbiont/foraminifera size ratio ψ (Eqn. 12) to characterise the symbiont affinity in taking up nutrients and light. Photomicrograph observations showed that foraminifera symbionts are about 1:20 smaller in size than the host cell (Takagi et al., 2019).

$$V_s = \psi^3 V_h \tag{12}$$

b. Symbionts' inorganic nutrient uptake

The generic nutrient uptake of symbionts follows a mixotrophy- (λ_s), quota- ($Q_{i_r}^{\text{stat}}$) and temperature-limited (γ_T) Michaelis-Menten function where the variable (**R**) represents nutrient resources and half-saturation constant is replaced by nutrient affinity, a more mechanistic parameter for nutrient uptake α. Nutrient affinity is often referred as "clearance rate" and regarded as a proxy of competitive strength (Fiksen et al., 2013). According to Edwards et al., (2012)' s review on phytoplankton trait trade-offs, scaled nutrient affinity is negatively related to cell size because of lower surface to volume ratio, while maximum uptake rate (V_m) is positively related.

$$V_{i_r} = \lambda_s \cdot Q_{i_r}^{\text{stat}} \cdot \gamma_T \cdot \frac{V_{i_r}^m \alpha_{i_r} \mathbf{R}}{V_{i_r}^m + \alpha_{i_r} \mathbf{R}} \tag{13}$$

c. Symbionts' photosynthesis

The symbionts' photosynthesis growth is modelled following the size-dependent unimodal equation (Geider et al., 1998; Moore et al., 2001) [OBJ], which has shown significant explanatory power for eukaryotes phytoplankton cells than power law (Bec et al., 2008). The maximum photosynthesis rate P_C^m is determined by dimensionless parameter P_a, P_b, P_c and the biovolume of symbiont V_s, and the mixotrophy cost λ_s.

$$P_C^m = \frac{\lambda_s (P_a + log_{10} V_s)}{P_b + P_c log_{10} V_s + log_{10} V_s^2} \tag{14}$$

The practical photosynthesis rate is further constrained by nutrient availability (the smallest between γ_{Fe} and γ_P), temperature (γ_T), light intensity (γ_I).

$$P_C = P_C^m \cdot \min[\gamma_P, \gamma_{Fe}] \cdot \gamma_T \cdot \gamma_I \tag{15}$$

https://doi.org/10.5194/gmd-2022-177
Preprint. Discussion started: 22 August 2022

Geoscientific Model Development Discussions

The nutrient limitation γ_{i_r} (i_r is either P or Fe, see the definition in Eqn. 2) takes the minimal value from phosphorus or iron limitation term, which follows the quota relationship in Droop (1968).

$$\gamma_{i_r} = \frac{1 - Q_{i_r}^{\min}/Q_{i_r}}{1 - Q_{i_r}^{\min}/Q_{i_r}^{\max}}, \quad i_r = \text{Fe, P} \tag{16}$$

As for the light limitation, it follows Moore et al., (2001) model where ***I*** represents light intensity, α is initial slope of P-I curve limited by Fe content (γ_{Fe}), and Q_{Chl} is chlorophyll quota.

$$\gamma_I = 1 - \exp\left(\frac{-\alpha \cdot \gamma_{Fe} \cdot Q_{\text{Chl}} \cdot I}{P_C^m \cdot \gamma_T \cdot \min[\gamma_P, \gamma_{Fe}]}\right) \tag{17}$$

d. Foraminifer predation cost

As a cost for symbiosis, we assume that having photosynthetic symbionts results in reducing foraminifer grazing rate (λ_h, Eqn. 7). Despite no direct and sufficient evidence for such a cost, this assumption is common practice in mixotroph models (Castellani et al., 2013; Våge et al., 2013; Ward and Follows, 2016).

2.5 Approximating foraminifera carbon production and export

Planktic foraminifera produce organic carbon in the subsurface water column (Salter et al., 2014) and sequester tests of inorganic carbon into the deep oceans (Schiebel, 2002). In the model we estimate organic carbon flux and approximate calcite export using an empirical converting factor (Schiebel and Movellan, 2012) as previous model implementations (Grigoratou et al., 2021a).

2.5.1 Organic Carbon Export

Foraminifera's organic carbon flux (F) comes from the mortality loss and predators' messy feeding (Eqn. 18).

$$\begin{aligned} F = & \sum_{j_{\text{foram}}=1, j_{\text{pred}}=1}^{J} \left(1 - \beta_{j_{\text{foram}}}\right)\left(1 - \lambda_{j_{\text{pred}}}\right) G_{j_{\text{pred}}, j_{\text{foram}}} B_{j_{\text{pred}}} \\ & + \sum_{j_{\text{foram}}=1}^{J} \left(1 - \beta_{j_{\text{foram}}}\right) m_{j_{\text{foram}}} B_{j_{\text{foram}}} \end{aligned} \tag{18}$$

$\beta_{j_{\text{foram}}}$ is the fraction of foraminiferal dissolved organic carbon (DOC) subject to advection by ocean circulation, and the remaining fraction is the particulate organic carbon (POC) subject to redistribution through the water column by sinking. Parameter β is defined by a size-based sigmoid function depending on maximum and minimum DOC fraction (β_{max}, β_{min}), and the size β_s at which DOC/POC ratio equals 1 (Ward and Follows, 2016). The proportion of DOC therefore decreases with plankton cell size.

$$\beta = \beta_{max} - \frac{\beta_{max} - \beta_{min}}{1 + \beta_s/ESD} \tag{19}$$

https://doi.org/10.5194/gmd-2022-177
Preprint. Discussion started: 22 August 2022

Geoscientific Model Development Discussions

Messy feeding behaviour is modelled as unassimilated carbon fraction ($1 - \lambda_{j_{pred}}$) of prey which is limited by the size-independent maximum efficiency coefficient (λ_m) and the nutrient limitation (Fe or P).

$$\lambda = \lambda_m \cdot min[Q_P^{stat}, Q_{Fe}^{stat}] \quad (20)$$

2.5.2 Calcite export

The model does not explicitly represent foraminifera calcification due to the poorly-understood mechanisms of calcification. Instead, we calculate a foraminifera $CaCO_3$ export by multiplying the foraminifera bulk organic carbon export with a rain-ratio. Here we use a globally uniform rain-ratio, based on the empirical first-order average ratio (0.36) between foraminifera-derived particle inorganic carbon (PIC) and organic carbon (POC) (Schiebel and Movellan, 2012) to approximate calcite export rate.

3 Model experiments and evaluation

3.1 Experiments

We set up the model plankton ecosystem to resolve eight size classes of phytoplankton, seven size classes of zooplankton and one size class for each of the four foraminifer groups. Phytoplankton and zooplankton size classes include 0.6, 1.9, 6.0, 19.0, 60.0, 190.0, 600.0 and 1900.0 µm. The foraminifer cell size is set to an Equivalent Sphere Diameter (ESD) of 190 µm, which is typical for an adult foraminifer (Grigoratou et al., 2019).

We run an ensemble of 1,200 model experiments, each testing a different combination of parameter values, to explore all possible trait values and select the best trait combinations to match the foraminifera observations (section 3.2).

We use a Latin Hypercube Sampling (LHS) algorithm to generate the 1,200 parameter combinations, sampling values of 12 model parameters characteristics of foraminifer traits (Table 2; Sarrazin et al., 2016). Each simulation is run for 250 years continuing from a 10,000-year spin-up simulation as ecosystem structure typically reaches equilibrium after ~50 years. The other ecosystem parameters are the same as Ward et al. (2018) (Table S3).

Table 2 List of the foraminifer-relevant parameters tested in the global sensitivity analysis (GSA) and identified parameter values for the best model run.

Foraminifer group*	Parameter	Description	GSA range†	Unit	Best model run
Symbiont-barren non-spinose	p_m	Protection from mortality	[0-1]		0.6

https://doi.org/10.5194/gmd-2022-177
Preprint. Discussion started: 22 August 2022


Geoscientific Model Development Discussions

	p_p	Protection from palatability	[0-1]		0.8
	r	Respiration rate	[0-0.02]	mmol C d^{-1}	0.01
	s	feeding behaviour (1=passive, 2=active)			1
	σ	standard deviation of prey range			2.0
Symbiont-barren spinose	ε	coefficient of grazing half saturation	[0-1]		0.9
	p_p	as above	[0-1]		0.7
	r	as above	[0-0.02]	mmol C d^{-1}	0.03
Symbiont-facultative non-spinose	ψ	symbiont: foraminifer size ratio	[0-0.05]		0.0015
	λ_s	symbiont autotroph discount	[0-1]		0.2
	λ_h	foraminifer heterotroph discount	[0-1]		0.8
Symbiont-bearing spinose	ψ	as above	[0-0.05]		0.0015
	λ_s	as above	[0-1]		0.7
	λ_h	as above	[0-1]		0.45

* For any other plankton group without these traits, scaling parameters are set to 1 and cost parameters are set to 0.

https://doi.org/10.5194/gmd-2022-177
Preprint. Discussion started: 22 August 2022

Geoscientific Model Development Discussions

† GSA range is set to [0-1] for scaling parameters; respiration terms are as follow Ward et al., (2018); symbiont cell size ratio is calculated from observation (Takagi et al., 2019).

295

3.2 Comparison to observations

To validate the foraminifera model, we compiled three global datasets of adult foraminifer (>150 μm) data: (1) plankton net tows mostly taken from the first 100 m, (2) core-top sediment representing the Late Holocene (pre-industrial) and (3) seasonally resolved sediment trap time-series. We use the core-top dataset of individual abundance count to validate the spatial patterns 300 of the relative proportion of each foraminifer group. We also use the ocean net tow (count m^{-3}) and sediment trap (count m^{-3} d^{-1}) datasets to validate the living stocks and carbon export of each group, respectively. The core-top data comes from ForCenS (Siccha and Kucera, 2017), and the plankton tow and sediment trap data from the compilation by Grigoratou, (2019) with additional foraminifera groups and sample sites. The full list of plankton tow and sediment trap data sources is in Tables S1 and S2.

305 We converted the plankton net tow and sediment trap data from "count m^{-3}" or "count m^{-3} d^{-1}" into "mmol C m^{-3}" or "mmol C m^{-3} d^{-1}" using the empirical factor of 0.845 μg $count^{-1}$ from Schiebel and Movellan (2012). We considered species with less than 3% abundance as absent to avoid the uncertainty caused by ocean currents transportation (van Sebille et al., 2015). We applied this threshold based on the standard error of fisher's α diversity index (Fisher et al., 1943). To further constrain the uncertainty of the observational data, we applied median absolute deviation (MAD) measurement to detect the most robust 310 and close-to-reality data. Finally, we grouped the species-based data into functional groups (Table 1) using species traits defined by Schiebel and Hemleben, (2017) and Takagi et al., (2019) (Table S2).

To compare with the sediment-trap and plankton tow time-series, we select sites with the most data points. For the time slice comparison, we re-gridd the observational data by averaging data in each model grid box.

We also perform basic statistics (mean, standard error, sum) on the model and observational data. We use the standard error 315 of the mean to represent the accuracy of the sampling mean, particularly for the observational studies. Finally, we do not consider model outputs for the Arctic and the Mediterranean Sea because of limitations with ocean physics due to low model resolution in that region.

3.3 Performance metrics

320 We calculate a M-score (Watterson, 2015) for each model experiment to quantify the model-data fit (Eqn. 19). This score spans from -1 to 1 with values closer to 1 representing better model performance.

$$M = \frac{2}{\pi} arcsin\left[\frac{\sum_{i=1}^{n}(M_i - O_i)^2 / n}{\sigma_m^2 + \sigma_o^2 + (\mu_m - \mu_o)^2}\right] \quad (21)$$

The numerator is mean square error, with M_i and O_i the model and observational value in the i^{th} grid, and n the total number of grids. σ^2 and μ are the variance and mean, with superscripts m and o representing model and observed fields, respectively.

325

https://doi.org/10.5194/gmd-2022-177
Preprint. Discussion started: 22 August 2022


Geoscientific Model Development Discussions

3.4 Global Sensitivity analysis

We conduct a global sensitivity analysis (GSA) to explore the model robustness of our 1,200 experiments using the PAWN method (Pianosi and Wagener, 2015). This method measures the sensitivity of model outputs (focusing on M-score here) to different values of input parameters. A total M-score is calculated by summing scores of each foraminifer group in biomass, POC flux, and relative abundance (i.e., the total score ranges from -12 to 12). To further measure the uncertainty and robustness of the GSA results, we also apply a bootstrapping method with 1,000 resamples. This method allows us to understand the confidence intervals of the sensitivity indices without running more experiments (Wagener and Pianosi, 2019),. We bootstrapped our data using *rsample* package (Silge et al., 2021) in the R software environment v4.1 (R Core Team, 2021).

4 Results and discussions

4.1 Model ensemble results

Overall, the 1,200 model runs fit generally reproduce POC export (M-score: -0.24 ~ 1.0) and relative abundance (M-score: -0.4 ~ 1.2), with poorer comparison with plankton net data (M-score: -0.14 ~ 0.14) (Figure 2). A heatmap of M-Scores (Figure 2) shows the experiments cluster into 5 groups with respect to the 3 observation metrics. Most clusters (A-D) show a trade-off between relative abundance and POC export performance, with either higher POC flux score but lower abundance score (cluster A, D), or *vice versa* (cluster C). Cluster E (which includes our best run) achieves the highest (best) abundance and POC export scores while showing the closest export rate to observations.

We select the run with the highest total M-score score, which also has the highest M-score for the relative abundance (group mean = 0.29) and POC flux (group mean = 0.18; Figure S1). We prioritise a higher score in relative abundance over POC flux and biomass because of better data quantity and quality in the top-core dataset. In this run, all the foraminifera groups except the symbiont-facultative non-spinose have the highest total M-score (Table 3). Compared to the EcoGENIE and ForamEcoGENIE 1.0, this set of parameters does not increase the overall ecosystem biomass or POC export, and slightly increases the mean cell size by ~0.5 μm (Figure 3c). Therefore, the incorporation of symbiosis and spines into our trait-based model successfully widens the ability of the model to represent foraminifers in the surface ocean by incorporating all four main foraminiferal ecogroups in the modern ocean without weakening the overall ability of predicting ecosystem body size, biomass and POC export.

https://doi.org/10.5194/gmd-2022-177
Preprint. Discussion started: 22 August 2022

Geoscientific Model Development
Discussions
Open Access
EGU

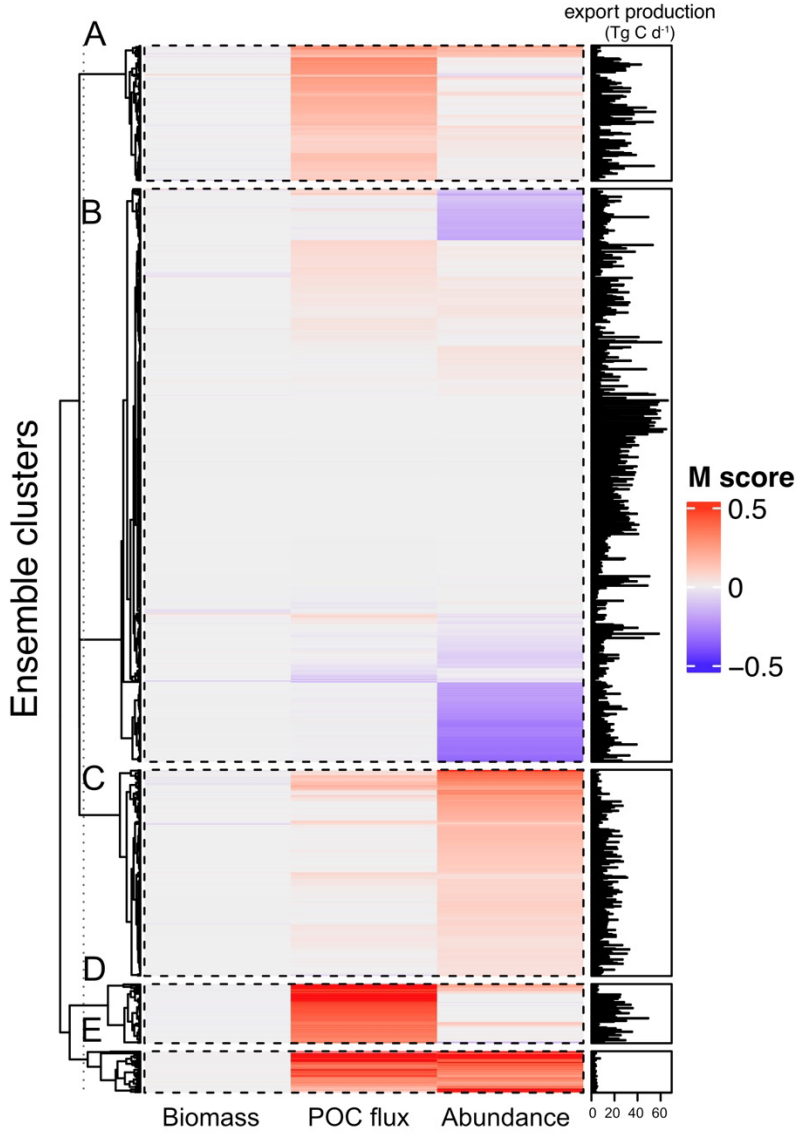

355 Figure 2. M-score heatmap of the model ensemble compared with foraminifera "Biomass" (plankton net data), "POC flux" (sediment trap data), groups' relative "Abundance" (sediment core top data). The right panel shows the global export production of all foraminifer groups. The ensemble cluster was derived from a complete linkage clustering algorithm (Jarman, 2020). The higher the M-score value the better the performance.

https://doi.org/10.5194/gmd-2022-177
Preprint. Discussion started: 22 August 2022

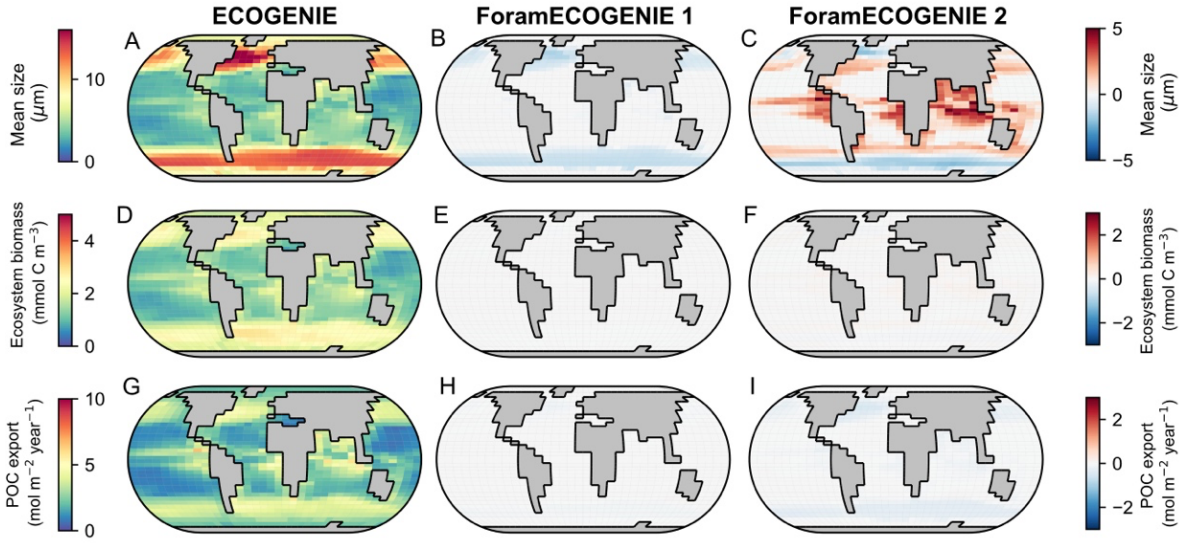

360

Figure 3. ForamEcoGENIE 2 best run (third column, with four foraminifer groups) comparison with ECOGENIE (first column) and ForamEcoGENIE 1 (second column, with non-spinose non-symbiont foraminifer only) in terms of ecosystem mean size, biomass and POC export. The first column displays absolute values, whilst the latter two are the anomaly compared with first column.

365

Table 3. Best model run for M-scores for a range of model outputs and the contribution of foraminiferal groups.

Groups	Symbiont-barren non-spinose	Symbiont-barren spinose	Symbiont-facultative non-spinose	Symbiont-obligate spinose	Column mean
Biomass	0.00	0.00	0.00	0.00	0.00
POC Export	0.19	0.28	0.09	0.15	0.18
Relative Abundance	0.42	0.31	0.05	0.38	0.29
Row Mean	0.20	0.30	0.05	0.18	

https://doi.org/10.5194/gmd-2022-177
Preprint. Discussion started: 22 August 2022


Geoscientific Model Development Discussions

370

4.2 Relative abundance distribution of foraminifer groups

Our best model run compares well with observations of core-top data showing the relative spatial distribution of the four foraminifera functional groups (Figure 4). The presence/absence pattern is also captured well in sediment trap and plankton net studies (Figure 5,6). The symbiont-obligate spinose group is the most abundant group with a global relative abundance of 375 43.2% (M-score: 0.38) dominating in the tropical open oceans, while the symbiont-barren non-spinose and spinose groups mainly occupy the high latitudes (M-score = 0.42 and 0.31, respectively). The symbiont-facultative group is not well captured with model-data disparities in the eastern equatorial pacific where the sediment core shows exclusively high abundance. This may be due to the resistant dissolution of some species' test (e.g., *N. dutertrei*) as suggested in a previous model study (Lombard et al., 2011). Overall, the Root Mean Square Error (RMSE) of relative abundance in this model (12% to 32%, Table S3) is 380 comparable to the species-based models, like FORAMCLIM (5-23%, Lombard et al., 2011) and PLAFOM (22-25%, Fraile et al., 2009). This indicates that symbionts and spines are sufficient to explain the variance of geographic distribution.

https://doi.org/10.5194/gmd-2022-177
Preprint. Discussion started: 22 August 2022

Geoscientific Model Development Discussions
Open Access
EGU

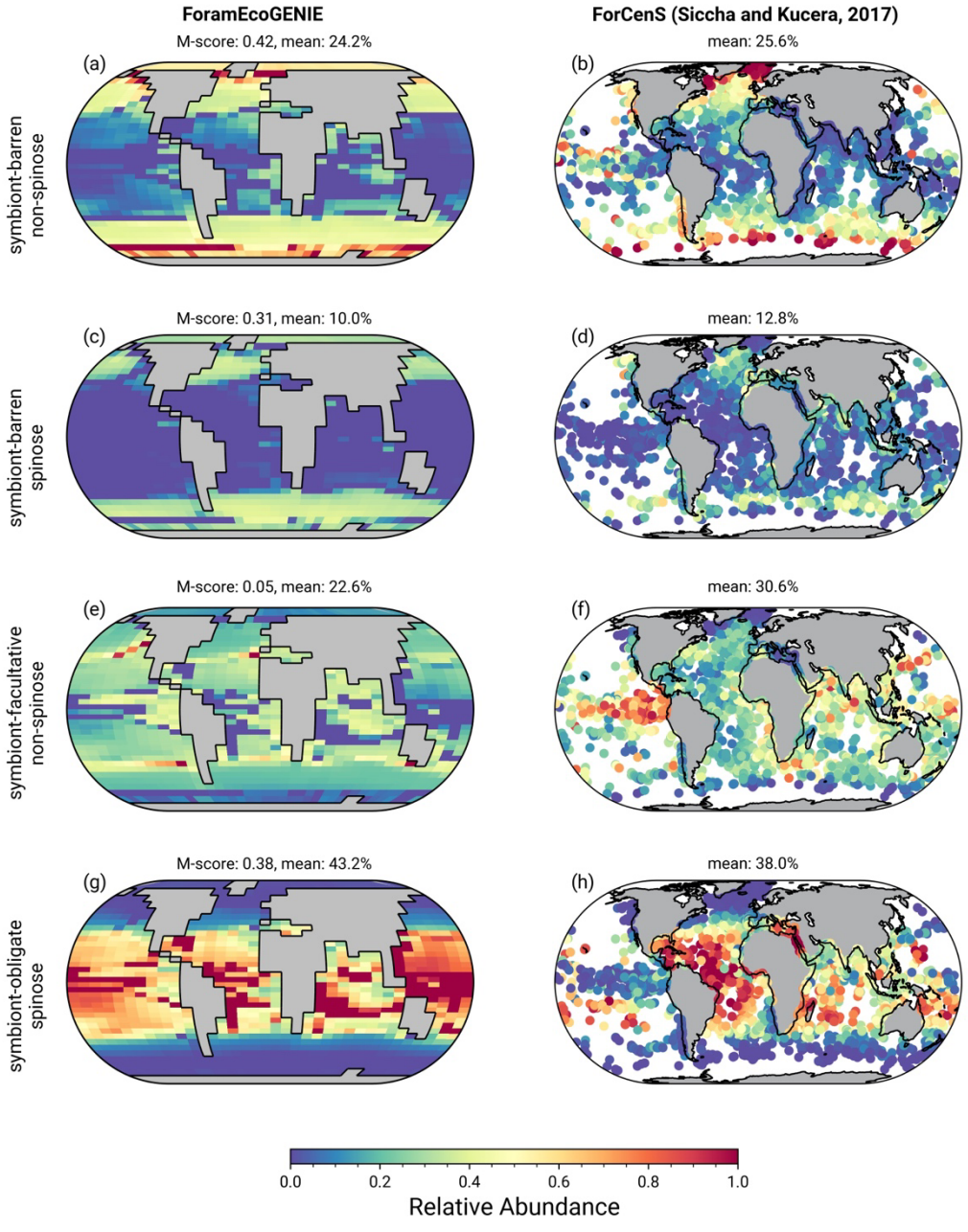

Figure 4. Relative abundance of the modelled geographical distribution (left column) of the four planktic foraminifer function groups, compared to the ForCenS core-top dataset (right column; Siccha and Kucera, 2017). Subplots titles are the M-scores
385 derived relative to observation and the global mean of relative abundance. Model relative abundance of each group are calculated based on POC flux rates.

https://doi.org/10.5194/gmd-2022-177
Preprint. Discussion started: 22 August 2022

Geoscientific Model Development Discussions

4.3 Living biomass of foraminifera groups

Although the general distribution pattern of foraminifera living biomass agrees with the observations from plankton nets (Figure 4), the corresponding M-scores are close to 0, indicating the model's inability in reproducing the living biomass magnitude of plankton net data. Our model overestimates the observed biomass on average by 0.02 mmol C m^{-3} (Figures 5 and 7a) or around 8 times. The model estimates a total of 32.3 TgC foraminifer organic carbon biomass, with symbiont-barren non-spinose taxa contributing the most (32.1%, or 10.3 TgC) (Figure 3c). For comparison, the MAREDAT dataset estimated the global mean living biomass of 0.0024 mmol C m^{-3} and the total of 0.94~3.63 TgC living foraminifer (with all groups included), with the production rate of 8.2–32.7 TgC yr^{-1} (Schiebel and Movellan, 2012). This indicates more foraminifer biomass are grazed by higher trophic levels than the model predicts because of the generally higher carbon export rate particularly for non-spinose foraminifera (Figure 7; see next section).

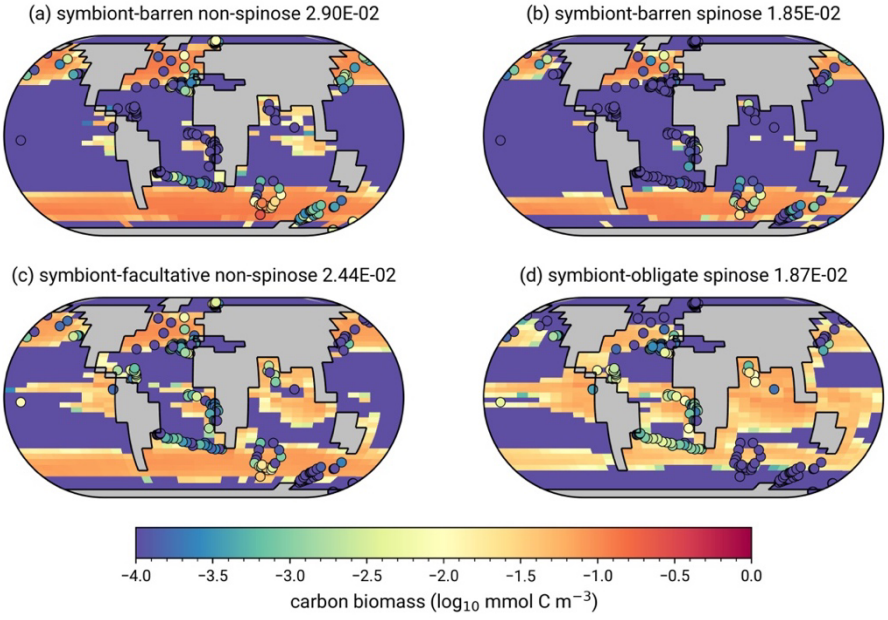

Figure 5. Model outputs of living biomass (mmol C m^{-3}) in log-10 scale compared with plankton net data (dots) for the four main functional groups of planktonic foraminifera.

4.4 POC and calcite export of foraminifera groups

The model reproduces consistent geographical distributions and magnitude of POC fluxes compared to sediment trap samples (Figure 6). The modelled mean POC flux rate is close to the collected trap observations for spinose foraminifers (Figure 7) but overestimates the POC flux of non-spinose foraminifer ~4 times. The mean M-score for the model POC flux is around 0.2,

https://doi.org/10.5194/gmd-2022-177
Preprint. Discussion started: 22 August 2022

Geoscientific Model Development Discussions

with the symbiont-baren spinose group performing the best (0.28) and the symbiont-facultative group performing the worst. The worse performance of non-spinose foraminifer is likely caused by over protection of test from grazing.

In terms of global estimation, the model suggests the organic carbon export of 365.3 TgC yr^{-1}. Symbiont-barren non-spinose taxa dominate this carbon export (141.7 TgC yr^{-1}) followed by symbiont-barren spinose, symbiont-facultative and symbiont-obligate groups (93.2, 83.1 and 47.3 TgC yr^{-1}, respectively). Using a converting mass ratio of 1:3 from organic carbon to calcium carbonate (Schiebel and Movellan, 2012), our model estimates a total calcite flux of pelagic foraminifera of 1.1 Gt $CaCO_3$ yr^{-1} comparable to the 1.3-3.2 Gt yr^{-1} of Schiebel (2002) within the top 100-m ocean. The calcite export in the model falls within the low range of previous estimates (1.3-3.2 Gt yr^{-1}; Schiebel et al., 2001) and contributes 19% to the global marine $CaCO_3$ production (Milliman et al., 1999). This estimate is similar to 21% reported in Kiss et al., (2021) based on sediment traps at Cape Blanc and to Salmon et al., (2015) data from the Sargasso Sea ranging between 0-40 % (but mostly < 25%). Regionally higher contributions (32-49%) have been reported in the Southern Ocean (Salter et al., 2014) who included deep-dwelling species which are not represented in this model. To summarise, our estimation of foraminifer calcite export is generally trustable to previous observational studies.

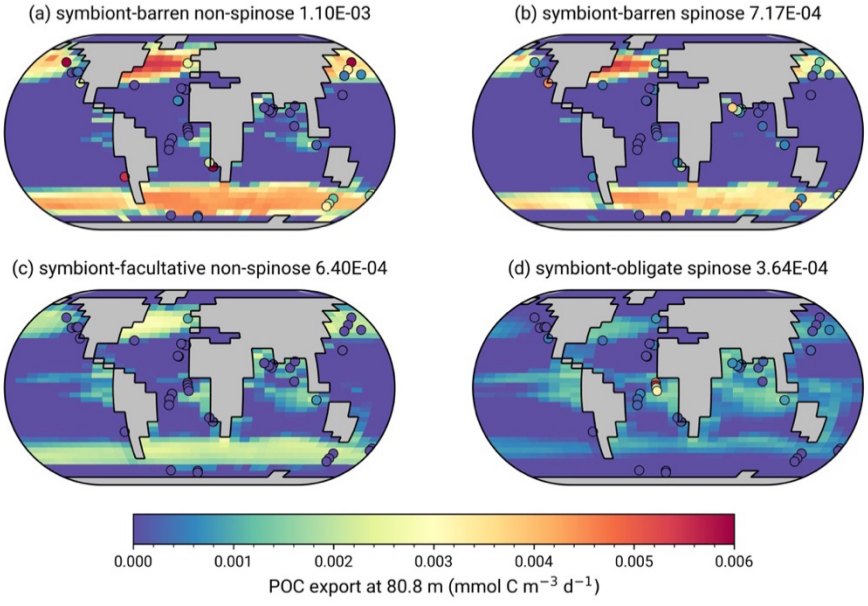

Figure 6. Model outputs of POC flux (mmol C m^{-3} d^{-1}) below the euphoric zone (80.8 m) in comparison to sediment trap samples (dots).

https://doi.org/10.5194/gmd-2022-177
Preprint. Discussion started: 22 August 2022

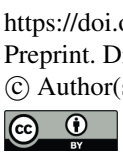

Geoscientific Model Development Discussions

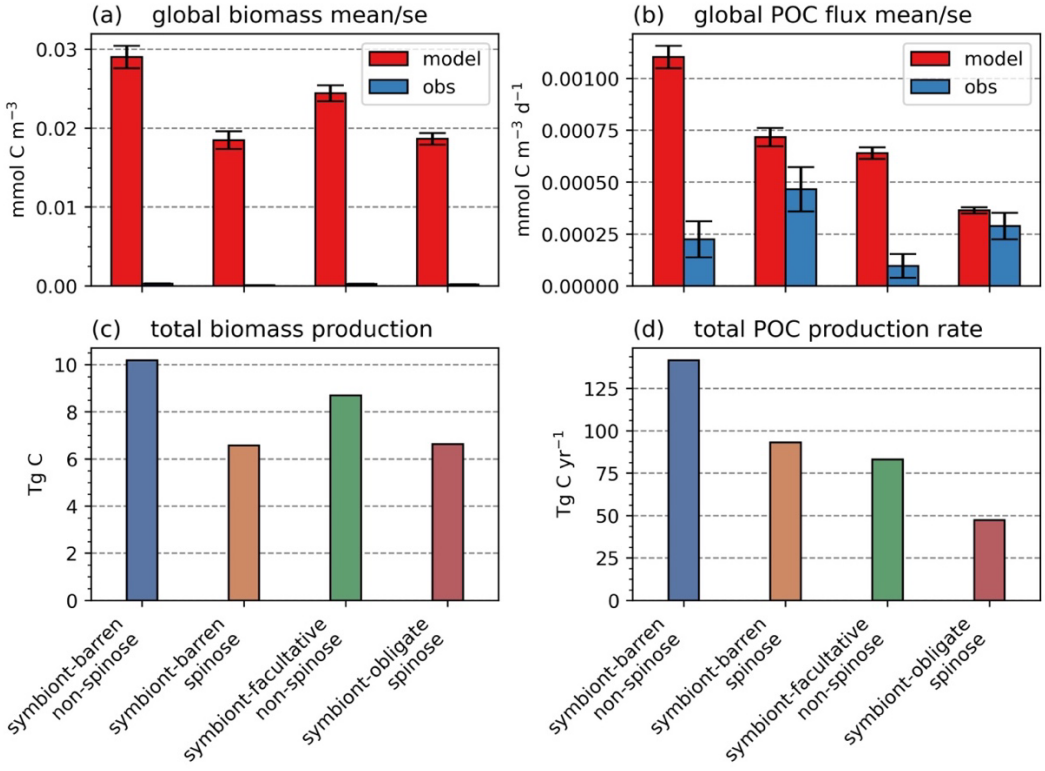

425 Figure 7. Summary of the modelled living biomass and POC export produced by the four foraminifer groups. (a) The modelled (red) and observational (blue) biomass (mmol C m^{-3}) and (b) POC flux rate below the euphotic zone (mmol C m^{-3} d^{-1}). Bar height and error bar represents spatial mean value and standard error, respectively. (c) A global estimation of modelling total carbon biomass (Tg) and (d) POC export rate (TgC yr^{-1}).

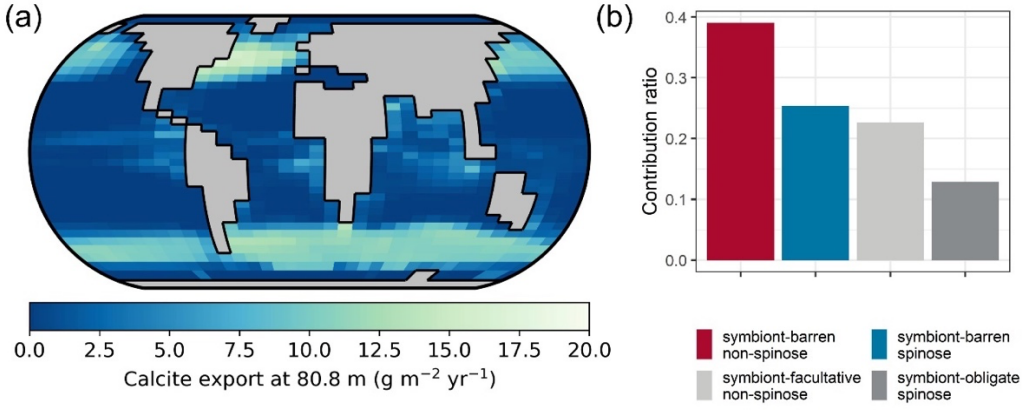

430 Figure 8. Global model estimates of (a) surface foraminiferal calcite flux rate (at 80.8 m; g m^{-2} yr^{-1}) and (b) group contribution.

https://doi.org/10.5194/gmd-2022-177
Preprint. Discussion started: 22 August 2022

4.5 Seasonal variations of foraminifera living biomass and POC export

The model-derived seasonality of foraminifera biomass and POC export are compared with observations in Figure 9 and 10. The model successfully reproduces the first-order seasonal patterns observed by sediment trap data at a basin scale, with low export and seasonality in open ocean locations such as the western Atlantic and the Sargasso Sea, summer blooms in the low latitudes (NW Pacific, Ocean Papa Station, Bay of Bengal) and spring blooms in high latitude (Subantarctic Zone). These results are generally consistent with PLAFOM (Fraile et al., 2008) despite species-specific discrepancy. The model does not reproduce biomass change in some upwelling and polar regions (e.g., Arabian Sea, Ross Sea) likely due to the low model resolution.

An additional source of uncertainty is the data quality, as ideally models should be calibrated against spatially and temporally abundant and well-constrained data. Therefore, the comparison of our model against plankton tow data was limited by the low temporal resolution of the data (Figure 9). The data is not only undersampled in limited regions (North Atlantic Ocean, Caribbean, Sea Arabian Sea) but also biased towards specific sampling seasons, generated using different mesh size and water depth as discussed in the first application of ForamEcoGENIE (Grigoratou et al., 2021a).

Parameter sensitivity test

We conducted a sensitivity analysis to determine which parameters influence the model performance most. The results show that the model performance is mostly sensitive to the symbiosis trait (λ_s), and the palatability protection (P_p) from both spine and calcification (Figure 10), confirming the important role of symbiosis and protection from predators in foraminiferal ecology and the possibility that overestimated biomass of non-spinose foraminifer is influenced by the palatability parameterisation.

https://doi.org/10.5194/gmd-2022-177
Preprint. Discussion started: 22 August 2022

Geoscientific Model Development Discussions

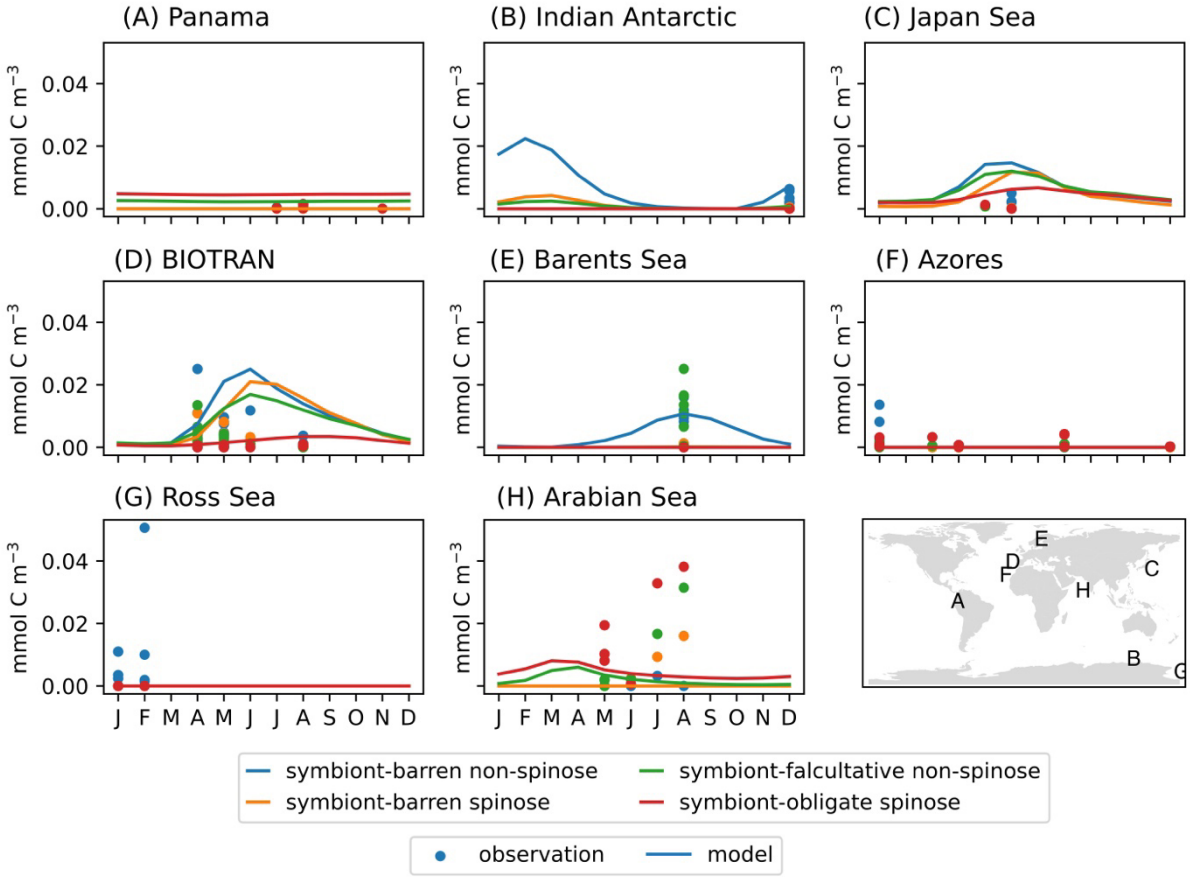

Figure 9. Biomass seasonal comparison between the model (lines) and observations (dots) (mmol C m^{-3}) in example locations (shown in the map with corresponding letter). Sites are selected to according to the number of comparable data points and ocean basins.

https://doi.org/10.5194/gmd-2022-177
Preprint. Discussion started: 22 August 2022

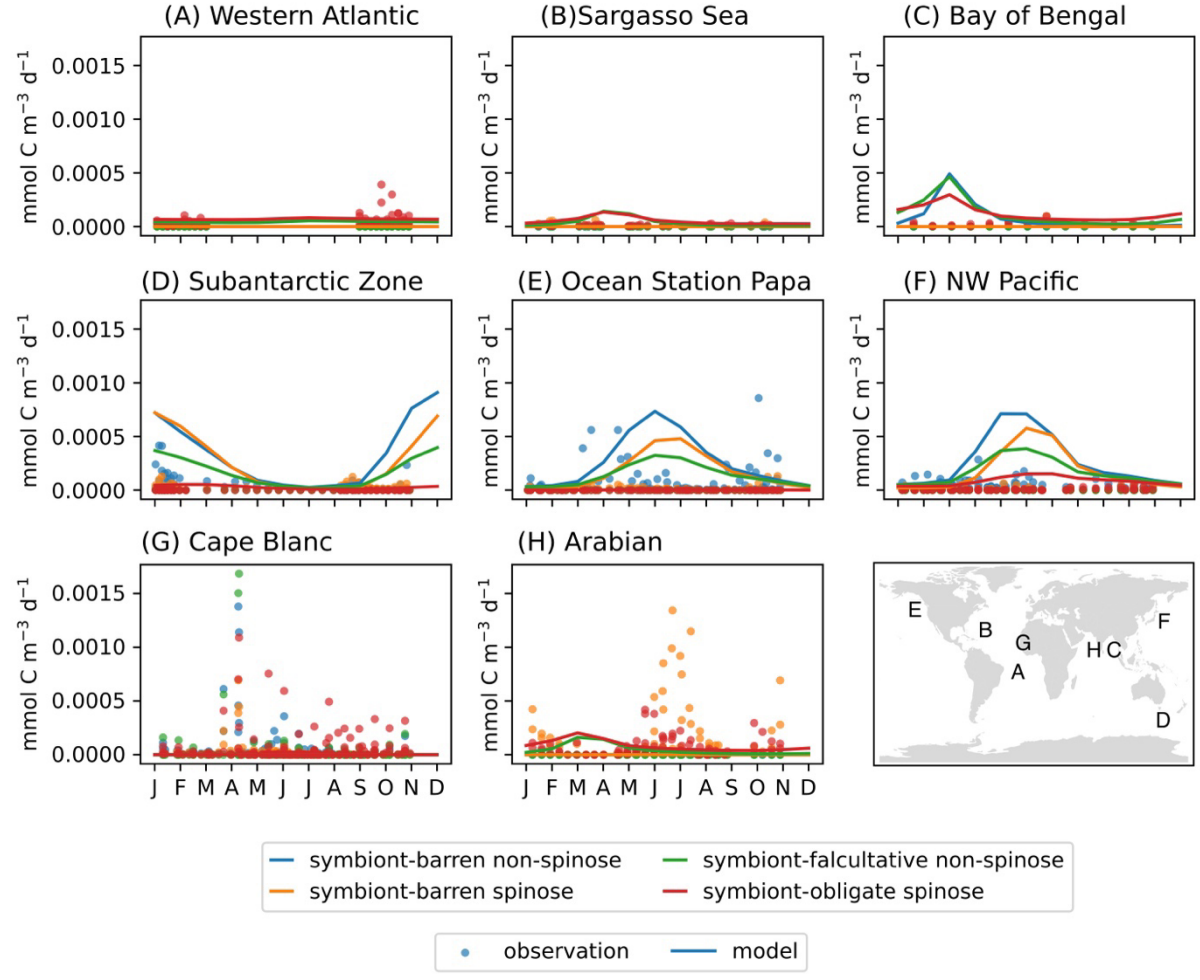

Figure 10. POC flux seasonal comparison between the model (lines) and observations (dots) (mmol C m^{-3} d^{-1}) in example sites (shown in the map with corresponding letter). Sites are selected to according to the number of comparable data points and ocean basins.

https://doi.org/10.5194/gmd-2022-177
Preprint. Discussion started: 22 August 2022

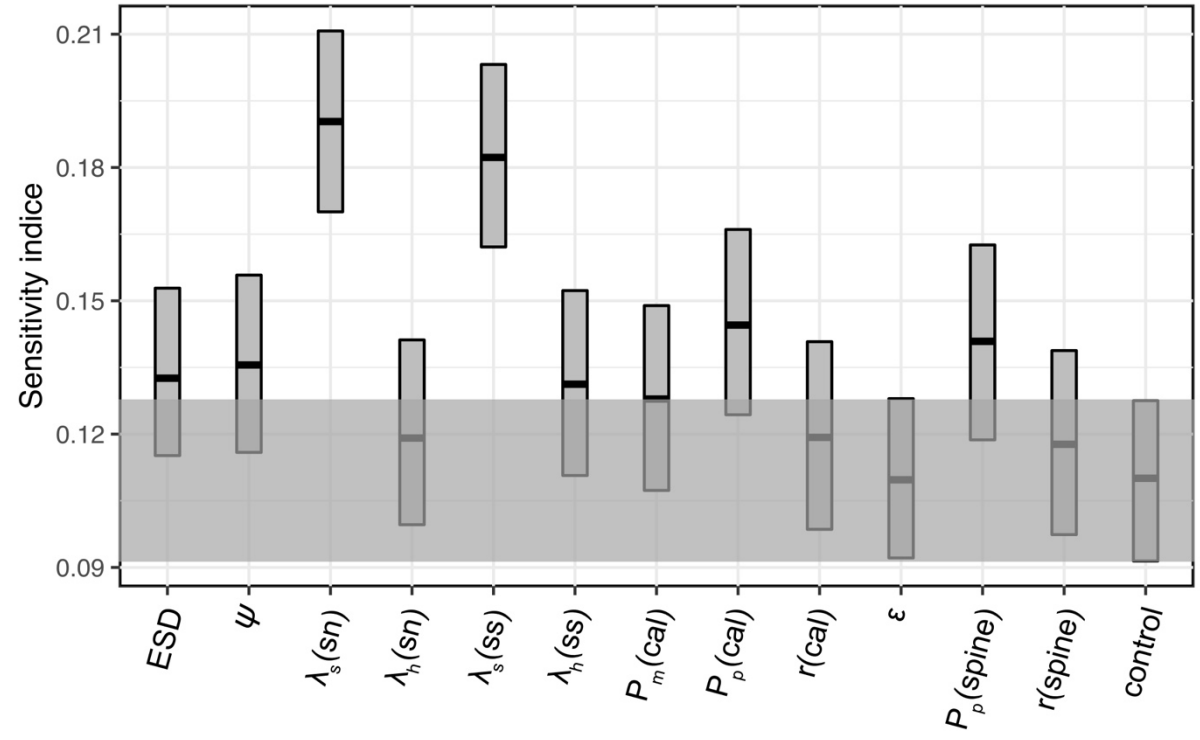

Figure 11. Sensitivity of parameters to overall model performance (as combined M-scores). Bar boundaries indicate the 95-percent confidence interval with the thick line showing the mean value. Grey area indicates non-influential range of index value as control group. sn, symbiont-facultative non-spinose; ss, symbiont-bearing spinose.

5 Model limitation

The limitations in our current trait understanding still influence our model definition and performance. For example, symbiotic spinose foraminifer can use their spines to place algal symbionts in the daytime (LeKieffre et al., 2018), which theoretically increases photosynthesis efficiency due to an increase in surface area relative to non-spinose species. In this model, we do not explicitly model the photosymbiotic relationships which could be sensitive to individual climate sensitivities of symbiont and host. Similarly, spinose foraminifera prefer large zooplankton prey over phytoplankton as their prey, while non-spinose species are often herbivorous (Anderson et al., 1979). Such specialised behaviour is not resolved in the model and might explain why the symbiont-barren spinose *G. bulloides* do not show opportunistic behaviour, i.e., appear earlier than other groups in the seasonal succession (Taylor et al., 2018; Schiebel et al., 2001).

https://doi.org/10.5194/gmd-2022-177
Preprint. Discussion started: 22 August 2022


Geoscientific Model Development Discussions

6 Summary

In this study, we extend the trait-based planktic foraminifer model, ForamEcoGENIE, to include symbiosis and spine traits and resolve all main foraminifer functional groups. Using Latin Hypercube Sampling, we generated 1,200 parameter samples and compared these with three global observational sources: core-top, plankton tow, sediment trap. We assessed the model performance of biogeographic distributions, the carbon biomass and carbon export. Our global sensitivity analysis shows the symbiosis trait and the palatability protection of spine and test strongly influence model performance. Despite overestimating the overall biomass, our best set of model parameters successfully reproduces the modern biogeographical distribution of the main four foraminifera ecogroups and produces a global mean organic carbon export similar to observations of 365.3 TgC yr^{-1}. The two symbiont-barren groups account for 64% of standing stocks and carbon export, while the two symbiotic group contribute the remaining 36%. The model accurately reproduces seasonal time-series observations of foraminiferal biomass and organic carbon flux in large parts of the ocean but performs poorly in upwelling regions, probably due to the low model resolution. The model suggests a foraminifera calcite export rate of 1.1 Gt yr^{-1}, equivalent to 19% of the global marine calcium carbonate budget. The value agrees with the lower end of modern estimates. These results provide confidence in the model's ability to explore foraminifer ecology and diversity in the geological record and to interpret and question the foraminifer microfossil records, for example of the last glacial maximum, as well as helping to solve riddles about their ecology in the past. The trait-based framework of cGENIE ecosystem also provides potential to extend the model by presenting more traits such as life history and differential calcification rates across groups.

Code and data availability

The source codes are archived in https:10.5281/zenodo.6808761. Experiment configuration and observational dataset can be found in genie-userconfig/MS/yingetal.GMD.2022.

Author contribution

RY, FMM, JDW, DNS designed the study. RY, FMM, JDW developed the model code. RY performed the experiments, data collection and visualisation. All authors wrote and edited the original draft.

Competing interests

The authors declare that they have no conflict of interest.

Acknowledgements

We acknowledge funding from Royal Society Wolfson Research Merit Award (DNS), NERC (NE/P019439/1 for DNS and JDW), NE/N011708/1 (FMM), TMS Angelina Messina Grant (RY), China Scholarship Council (RY, No. 202006380070), and AXA Research Fund Postdoctoral Fellowship (JDW). We would like to thank Maria Grigoratou for her insights on the model development.

https://doi.org/10.5194/gmd-2022-177
Preprint. Discussion started: 22 August 2022

References

Adloff, M., Ridgwell, A., Monteiro, F. M., Parkinson, I. J., Dickson, A. J., Pogge von Strandmann, P. A. E., Fantle, M. S., and Greene, S. E.: Inclusion of a suite of weathering tracers in the cGENIE Earth system model – muffin release v.0.9.23, Geosci. Model Dev., 14, 4187–4223, https://doi.org/10.5194/gmd-14-4187-2021, 2021.

Andersen, K. H., Berge, T., Gonçalves, R. J., Hartvig, M., Heuschele, J., Hylander, S., Jacobsen, N. S., Lindemann, C., Martens, E. A., Neuheimer, A. B., Olsson, K., Palacz, A., Prowe, A. E. F., Sainmont, J., Traving, S. J., Visser, A. W., Wadhwa, N., and Kiørboe, T.: Characteristic Sizes of Life in the Oceans, from Bacteria to Whales, 8, 217–241, https://doi.org/10/f3pdzr, 2016.

Anderson, O. R. and Bé, A. W. H.: The ultrastructure of a planktonic foraminifer, Globigerinoides sacculifer (Brady), and its symbiotic dinoflagellates, Journal of Foraminiferal Research, 6, 1–21, https://doi.org/10.2113/gsjfr.6.1.1, 1976.

Anderson, O. R., Spindler, M., Bé, A. W. H., and Hemleben, Ch.: Trophic activity of planktonic foraminifera, J. Mar. Biol. Ass., 59, 791–799, https://doi.org/10.1017/S002531540004577X, 1979.

Aumont, O., Ethé, C., Tagliabue, A., Bopp, L., and Gehlen, M.: PISCES-v2: an ocean biogeochemical model for carbon and ecosystem studies, 8, 2465–2513, https://doi.org/10.5194/gmd-8-2465-2015, 2015.

Bec, Bé., Collos, Y., Vaquer, A., Mouillot, D., and Souchu, P.: Growth rate peaks at intermediate cell size in marine photosynthetic picoeukaryotes, Limnol. Oceanogr., 53, 863–867, https://doi.org/10.4319/lo.2008.53.2.0863, 2008.

Brovkin, V., Brücher, T., Kleinen, T., Zaehle, S., Joos, F., Roth, R., Spahni, R., Schmitt, J., Fischer, H., Leuenberger, M., Stone, E. J., Ridgwell, A., Chappellaz, J., Kehrwald, N., Barbante, C., Blunier, T., and Dahl Jensen, D.: Comparative carbon cycle dynamics of the present and last interglacial, Quaternary Science Reviews, 137, 15–32, https://doi.org/10.1016/j.quascirev.2016.01.028, 2016.

Brown, J. H., Gillooly, J. F., Allen, A. P., Savage, V. M., and West, G. B.: Toward a Metabolic Theory of Ecology, 1771–1789, https://doi.org/10.1890/03-9000@10.1002/(ISSN)1939-9170.MacArthurAward, 2004.

Buitenhuis, E. T., Vogt, M., Moriarty, R., Bednaršek, N., Doney, S. C., Leblanc, K., Le Quéré, C., Luo, Y.-W., O'Brien, C., O'Brien, T., Peloquin, J., Schiebel, R., and Swan, C.: MAREDAT: towards a world atlas of MARine Ecosystem DATa, 5, 227–239, https://doi.org/10.5194/essd-5-227-2013, 2013.

Buitenhuis, E. T., Quéré, C. L., Bednaršek, N., and Schiebel, R.: Large Contribution of Pteropods to Shallow CaCO3 Export, 33, 458–468, https://doi.org/10/gjpnzt, 2019.

Cao, L., Eby, M., Ridgwell, A., Caldeira, K., Archer, D., Ishida, A., Joos, F., Matsumoto, K., Mikolajewicz, U., Mouchet, A., Orr, J. C., Plattner, G.-K., Schlitzer, R., Tokos, K., Totterdell, I., Tschumi, T., Yamanaka, Y., and Yool, A.: The role of ocean transport in the uptake of anthropogenic CO2, Biogeosciences, 6, 375–390, https://doi.org/10/fp96kf, 2009.

Caromel, A. G. M., Schmidt, D. N., Fletcher, I., and Rayfield, E. J.: Morphological Change During The Ontogeny Of The Planktic Foraminifera, Journal of Micropalaeontology, 2014–017, https://doi.org/10.1144/jmpaleo2014-017, 2015.

Castellani, M., Våge, S., Strand, E., Thingstad, T. F., and Giske, J.: The Scaled Subspaces Method: A new trait-based approach to model communities of populations with largely inhomogeneous density, Ecological Modelling, 251, 173–186, https://doi.org/10.1016/j.ecolmodel.2012.12.006, 2013.

Daniels, C. J., Poulton, A. J., Balch, W. M., Marañón, E., Adey, T., Bowler, B. C., Cermeño, P., Charalampopoulou, A., Crawford, D. W., Drapeau, D., Feng, Y., Fernández, A., Fernández, E., Fragoso, G. M., González, N., Graziano, L. M.,

Heslop, R., Holligan, P. M., Hopkins, J., Huete-Ortega, M., Hutchins, D. A., Lam, P. J., Lipsen, M. S., López-Sandoval, D. C., Loucaides, S., Marchetti, A., Mayers, K. M. J., Rees, A. P., Sobrino, C., Tynan, E., and Tyrrell, T.: A global compilation of coccolithophore calcification rates, Earth Syst. Sci. Data, 10, 1859–1876, https://doi.org/10.5194/essd-10-1859-2018, 2018.

Droop, M. R.: Vitamin B12 and Marine Ecology. IV. The Kinetics of Uptake, Growth and Inhibition in Monochrysis Lutheri, J. Mar. Biol. Ass., 48, 689–733, https://doi.org/10.1017/S0025315400019238, 1968.

Edwards, K. F., Thomas, M. K., Klausmeier, C. A., and Litchman, E.: Allometric scaling and taxonomic variation in nutrient utilization traits and maximum growth rate of phytoplankton, Limnol. Oceanogr., 57, 554–566, https://doi.org/10.4319/lo.2012.57.2.0554, 2012.

Edwards, N. R. and Marsh, R.: Uncertainties due to transport-parameter sensitivity in an efficient 3-D ocean-climate model, Clim Dyn, 24, 415–433, https://doi.org/10/fcvq9k, 2005.

Enquist, B. J., Norberg, J., Bonser, S. P., Violle, C., Webb, C. T., Henderson, A., Sloat, L. L., and Savage, V. M.: Chapter Nine - Scaling from Traits to Ecosystems: Developing a General Trait Driver Theory via Integrating Trait-Based and Metabolic Scaling Theories, in: Advances in Ecological Research, vol. 52, edited by: Pawar, S., Woodward, G., and Dell, A. I., Academic Press, 249–318, https://doi.org/10.1016/bs.aecr.2015.02.001, 2015.

Ezard, T. H. G., Aze, T., Pearson, P. N., and Purvis, A.: Interplay Between Changing Climate and Species' Ecology Drives Macroevolutionary Dynamics, 332, 349–351, https://doi.org/10/bd77gm, 2011.

Fiksen, Ø., Follows, M. J., and Aksnes, D. L.: Trait-based models of nutrient uptake in microbes extend the Michaelis-Menten framework, Limnol. Oceanogr., 58, 193–202, https://doi.org/10.4319/lo.2013.58.1.0193, 2013.

Fisher, R. A., Corbet, A. S., and Williams, C. B.: The Relation Between the Number of Species and the Number of Individuals in a Random Sample of an Animal Population, 12, 42–58, https://doi.org/10.2307/1411, 1943.

Flynn, K. J.: The importance of the form of the quota curve and control of non-limiting nutrient transport in phytoplankton models, Journal of Plankton Research, 30, 423–438, https://doi.org/10.1093/plankt/fbn007, 2008.

Follows, M. J., Dutkiewicz, S., Grant, S., and Chisholm, S. W.: Emergent Biogeography of Microbial Communities in a Model Ocean, 315, 1843–1846, https://doi.org/10/bf6j95, 2007.

Fraile, I., Schulz, M., Mulitza, S., and Kucera, M.: Predicting the global distribution of planktonic foraminifera using a dynamic ecosystem model, 5, 891–911, https://doi.org/10/dkjgd3, 2008.

Fraile, I., Schulz, M., Mulitza, S., Merkel, U., Prange, M., and Paul, A.: Modeling the seasonal distribution of planktonic foraminifera during the Last Glacial Maximum, 24, https://doi.org/10/dh2z9t, 2009.

Geider, R. J., Maclntyre, H. L., and Kana, T. M.: A dynamic regulatory model of phytoplanktonic acclimation to light, nutrients, and temperature, Limnol. Oceanogr., 43, 679–694, https://doi.org/10.4319/lo.1998.43.4.0679, 1998.

Grigoratou, M.: A trait-based approach to planktonic foraminifera ecology and biogeography, University of Bristol, 2019.

Grigoratou, M., Monteiro, F. M., Schmidt, D. N., Wilson, J. D., Ward, B. A., and Ridgwell, A.: A trait-based modelling approach to planktonic foraminifera ecology, 16, 1469–1492, https://doi.org/10/gj349g, 2019.

Grigoratou, M., Monteiro, F. M., Wilson, J. D., Ridgwell, A., and Schmidt, D. N.: Exploring the impact of climate change on the global distribution of non-spinose planktonic foraminifera using a trait-based ecosystem model, Glob Change Biol, gcb.15964, https://doi.org/10.1111/gcb.15964, 2021a.

https://doi.org/10.5194/gmd-2022-177
Preprint. Discussion started: 22 August 2022

Grigoratou, M., Monteiro, F. M., Ridgwell, A., and Schmidt, D. N.: Investigating the benefits and costs of spines and diet on planktonic foraminifera distribution with a trait-based ecosystem model, Marine Micropaleontology, 102004, https://doi.org/10/gkbn65, 2021b.

Hemleben, C., Spindler, M., and Erson, O. R.: Modern planktonic foraminifera, 363 pp., 1989.

Henehan, M. J., Ridgwell, A., Thomas, E., Zhang, S., Alegret, L., Schmidt, D. N., Rae, J. W. B., Witts, J. D., Landman, N. H., Greene, S. E., Huber, B. T., Super, J. R., Planavsky, N. J., and Hull, P. M.: Rapid ocean acidification and protracted Earth system recovery followed the end-Cretaceous Chicxulub impact, PNAS, 116, 22500–22504, https://doi.org/10/ggbnrm, 2019.

Holling, C. S.: The Functional Response of Predators to Prey Density and its Role in Mimicry and Population Regulation, Mem. Entomol. Soc. Can., 97, 5–60, https://doi.org/10/fhjtms, 1965.

Hönisch, B., Ridgwell, A., Schmidt, D. N., Thomas, E., Gibbs, S. J., Sluijs, A., Zeebe, R., Kump, L., Martindale, R. C., Greene, S. E., Kiessling, W., Ries, J., Zachos, J. C., Royer, D. L., Barker, S., Marchitto, T. M., Moyer, R., Pelejero, C., Ziveri, P., Foster, G. L., and Williams, B.: The Geological Record of Ocean Acidification, Science, 335, 1058–1063, https://doi.org/10/gdj3zf, 2012.

Hurrell, J. W., Holland, M. M., Gent, P. R., Ghan, S., Kay, J. E., Kushner, P. J., Lamarque, J.-F., Large, W. G., Lawrence, D., Lindsay, K., Lipscomb, W. H., Long, M. C., Mahowald, N., Marsh, D. R., Neale, R. B., Rasch, P., Vavrus, S., Vertenstein, M., Bader, D., Collins, W. D., Hack, J. J., Kiehl, J., and Marshall, S.: The Community Earth System Model: A Framework for Collaborative Research, Bull. Amer. Meteor. Soc., 94, 1339–1360, https://doi.org/10.1175/BAMS-D-12-00121.1, 2013.

Jarman, A. M.: Hierarchical cluster analysis: Comparison of single linkage, complete linkage, average linkage and centroid linkage method, 2020.

Kiørboe, T., Visser, A., and Andersen, K. H.: A trait-based approach to ocean ecology, 75, 1849–1863, https://doi.org/10.1093/icesjms/fsy090, 2018.

Kiss, P., Jonkers, L., Hudáčková, N., Reuter, R. T., Donner, B., Fischer, G., and Kucera, M.: Determinants of Planktonic Foraminifera Calcite Flux: Implications for the Prediction of Intra- and Inter-Annual Pelagic Carbonate Budgets, Global Biogeochem Cycles, 35, https://doi.org/10.1029/2020GB006748, 2021.

Kretschmer, K., Jonkers, L., Kucera, M., and Schulz, M.: Modeling seasonal and vertical habitats of planktonic foraminifera on a global scale, 15, 4405–4429, https://doi.org/10/gdx3bj, 2018.

LeKieffre, C., Spero, H. J., Russell, A. D., Fehrenbacher, J. S., Geslin, E., and Meibom, A.: Assimilation, translocation, and utilization of carbon between photosynthetic symbiotic dinoflagellates and their planktic foraminifera host, Mar Biol, 165, 104, https://doi.org/10/gj35br, 2018.

Lombard, F., Labeyrie, L., Michel, E., Bopp, L., Cortijo, E., Retailleau, S., Howa, H., and Jorissen, F.: Modelling planktic foraminifer growth and distribution using an ecophysiological multi-species approach, 8, 853–873, https://doi.org/10.5194/bg-8-853-2011, 2011.

Marsh, R., Müller, S. A., Yool, A., and Edwards, N. R.: Incorporation of the C-GOLDSTEIN efficient climate model into the GENIE framework: “eb_go_gs” configurations of GENIE, 4, 957–992, https://doi.org/10.5194/gmd-4-957-2011, 2011.

Meyer, K. M., Kump, L. R., and Ridgwell, A.: Biogeochemical controls on photic-zone euxinia during the end-Permian mass extinction, Geol, 36, 747, https://doi.org/10.1130/G24618A.1, 2008.

https://doi.org/10.5194/gmd-2022-177
Preprint. Discussion started: 22 August 2022

Milliman, J. D., Troy, P. J., Balch, W. M., Adams, A. K., Li, Y.-H., and Mackenzie, F. T.: Biologically mediated dissolution of calcium carbonate above the chemical lysocline?, Deep Sea Research Part I: Oceanographic Research Papers, 46, 1653–1669, https://doi.org/10/fj6bq4, 1999.

Monteiro, F. M., Follows, M. J., and Dutkiewicz, S.: Distribution of diverse nitrogen fixers in the global ocean: DIVERSE NITROGEN FIXERS IN GLOBAL OCEAN, Global Biogeochem. Cycles, 24, n/a-n/a, https://doi.org/10/ctkc4h, 2010.

Moore, J. K., Doney, S. C., Kleypas, J. A., Glover, D. M., and Fung, I. Y.: An intermediate complexity marine ecosystem model for the global domain, Deep Sea Research Part II: Topical Studies in Oceanography, 49, 403–462, https://doi.org/10/bp99zn, 2001.

Morard, R., Garet-Delmas, M.-J., Mahé, F., Romac, S., Poulain, J., Kucera, M., and de Vargas, C.: Surface ocean metabarcoding confirms limited diversity in planktonic foraminifera but reveals unknown hyper-abundant lineages, Sci Rep, 8, 2539, https://doi.org/10.1038/s41598-018-20833-z, 2018.

Ortiz, J. D., Mix, A. C., and Collier, R. W.: Environmental control of living symbiotic and asymbiotic foraminifera of the California Current, Paleoceanography, 10, 987–1009, https://doi.org/10/ft8jc7, 1995.

Pianosi, F. and Wagener, T.: A simple and efficient method for global sensitivity analysis based on cumulative distribution functions, Environmental Modelling & Software, 67, 1–11, https://doi.org/10/f677qs, 2015.

R Core Team: R: A Language and Environment for Statistical Computing, R Foundation for Statistical Computing, Vienna, Austria, 2021.

Rae, J. W. B., Gray, W. R., Wills, R. C. J., Eisenman, I., Fitzhugh, B., Fotheringham, M., Littley, E. F. M., Rafter, P. A., Rees-Owen, R., Ridgwell, A., Taylor, B., and Burke, A.: Overturning circulation, nutrient limitation, and warming in the Glacial North Pacific, 6, eabd1654, https://doi.org/10/ghrj7m, 2020.

Renaud, S. and Schmidt, D. N.: Habitat tracking as a response of the planktic foraminifer Globorotalia truncatulinoides to environmental fluctuations during the last 140 kyr, Marine Micropaleontology, 49, 97–122, https://doi.org/10/bgp3cz, 2003.

Ridgwell, A. and Hargreaves, J. C.: Regulation of atmospheric CO_2 by deep-sea sediments in an Earth system model: REGULATION OF CO_2 BY DEEP-SEA SEDIMENTS, Global Biogeochem. Cycles, 21, n/a-n/a, https://doi.org/10.1029/2006GB002764, 2007.

Ridgwell, A. and Schmidt, D. N.: Past constraints on the vulnerability of marine calcifiers to massive carbon dioxide release, Nature Geosci, 3, 196–200, https://doi.org/10.1038/ngeo755, 2010.

Ridgwell, A., Hargreaves, J. C., Edwards, N. R., Annan, J. D., Lenton, T. M., Marsh, R., Yool, A., and Watson, A.: Marine geochemical data assimilation in an efficient Earth System Model of global biogeochemical cycling, Biogeosciences, 4, 87–104, https://doi.org/10/dcq62d, 2007.

Roy, T., Lombard, F., Bopp, L., and Gehlen, M.: Projected impacts of climate change and ocean acidification on the global biogeography of planktonic Foraminifera, 12, 2873–2889, https://doi.org/10/f7gcgw, 2015.

Salmon, K. H., Anand, P., Sexton, P. F., and Conte, M.: Upper ocean mixing controls the seasonality of planktonic foraminifer fluxes and associated strength of the carbonate pump in the oligotrophic North Atlantic, Biogeosciences, 12, 223–235, https://doi.org/10.5194/bg-12-223-2015, 2015.

Salter, I., Schiebel, R., Ziveri, P., Movellan, A., Lampitt, R., and Wolff, G. A.: Carbonate counter pump stimulated by natural iron fertilization in the Polar Frontal Zone, 7, 885–889, https://doi.org/10.1038/ngeo2285, 2014.

Sarrazin, F., Pianosi, F., and Wagener, T.: Global Sensitivity Analysis of environmental models: Convergence and validation, Environmental Modelling & Software, 79, 135–152, https://doi.org/10/f8n8kp, 2016.

Schiebel, R.: Planktic foraminiferal sedimentation and the marine calcite budget, 16, 3-1-3–21, https://doi.org/10/bdxfhs, 2002.

Schiebel, R. and Hemleben, C.: Planktic Foraminifers in the Modern Ocean, Springer Berlin Heidelberg, Berlin, Heidelberg, https://doi.org/10.1007/978-3-662-50297-6, 2017.

Schiebel, R. and Movellan, A.: First-order estimate of the planktic foraminifer biomass in the modern ocean, 4, 75–89, https://doi.org/10.5194/essd-4-75-2012, 2012.

Schiebel, R., Waniek, J., Bork, M., and Hemleben, C.: Planktic foraminiferal production stimulated by chlorophyll redistribution and entrainment of nutrients, 48, 721–740, https://doi.org/10/cnsg4p, 2001.

van Sebille, E., Scussolini, P., Durgadoo, J. V., Peeters, F. J. C., Biastoch, A., Weijer, W., Turney, C., Paris, C. B., and Zahn, R.: Ocean currents generate large footprints in marine palaeoclimate proxies, Nat Commun, 6, 6521, https://doi.org/10/f67xqv, 2015.

Siccha, M. and Kucera, M.: ForCenS, a curated database of planktonic foraminifera census counts in marine surface sediment samples, Sci Data, 4, 170109, https://doi.org/10.1038/sdata.2017.109, 2017.

Silge, J., Chow, F., Kuhn, M., and Wickham, H.: rsample: General resampling infrastructure, 2021.

Sunagawa, S., Acinas, S. G., Bork, P., Bowler, C., Eveillard, D., Gorsky, G., Guidi, L., Iudicone, D., Karsenti, E., Lombard, F., Ogata, H., Pesant, S., Sullivan, M. B., Wincker, P., and de Vargas, C.: Tara Oceans: towards global ocean ecosystems biology, Nat Rev Microbiol, 18, 428–445, https://doi.org/10.1038/s41579-020-0364-5, 2020.

Takagi, H., Kimoto, K., Fujiki, T., Saito, H., Schmidt, C., Kucera, M., and Moriya, K.: Characterizing photosymbiosis in modern planktonic foraminifera, 16, 3377–3396, https://doi.org/10/gj35bq, 2019.

Taylor, B. J., Rae, J. W. B., Gray, W. R., Darling, K. F., Burke, A., Gersonde, R., Abelmann, A., Maier, E., Esper, O., and Ziveri, P.: Distribution and ecology of planktic foraminifera in the North Pacific: Implications for paleo-reconstructions, Quaternary Science Reviews, 191, 256–274, https://doi.org/10/gdxpqh, 2018.

Tierney, J. E., Poulsen, C. J., Montañez, I. P., Bhattacharya, T., Feng, R., Ford, H. L., Hönisch, B., Inglis, G. N., Petersen, S. V., Sagoo, N., Tabor, C. R., Thirumalai, K., Zhu, J., Burls, N. J., Foster, G. L., Goddéris, Y., Huber, B. T., Ivany, L. C., Kirtland Turner, S., Lunt, D. J., McElwain, J. C., Mills, B. J. W., Otto-Bliesner, B. L., Ridgwell, A., and Zhang, Y. G.: Past climates inform our future, Science, 370, eaay3701, https://doi.org/10/gh6c3g, 2020.

Todd, C. L., Schmidt, D. N., Robinson, M. M., and Schepper, S. D.: Planktic Foraminiferal Test Size and Weight Response to the Late Pliocene Environment, 35, e2019PA003738, https://doi.org/10/ghrd4r, 2020.

Uhle, M. E., Macko, S. A., Spero, H. J., Lea, D. W., Ruddiman, W. F., and Engel, M. H.: The fate of nitrogen in the Orbulina universa foraminifera-symbiont system determined by nitrogen isotope analyses of shell-bound organic matter, Limnol. Oceanogr., 44, 1968–1977, https://doi.org/10/ffgtfw, 1999.

Våge, S., Castellani, M., Giske, J., and Thingstad, T. F.: Successful strategies in size structured mixotrophic food webs, Aquat Ecol, 47, 329–347, https://doi.org/10.1007/s10452-013-9447-y, 2013.

van de Velde, S. J., Hülse, D., Reinhard, C. T., and Ridgwell, A.: Iron and sulfur cycling in the cGENIE.muffin Earth system model (v0.9.21), Geosci. Model Dev., 14, 2713–2745, https://doi.org/10.5194/gmd-14-2713-2021, 2021.

https://doi.org/10.5194/gmd-2022-177
Preprint. Discussion started: 22 August 2022

Ward, B. A. and Follows, M. J.: Marine mixotrophy increases trophic transfer efficiency, mean organism size, and vertical carbon flux, Proc Natl Acad Sci USA, 113, 2958–2963, https://doi.org/10/ggnmm5, 2016.

Ward, B. A., Wilson, J. D., Death, R. M., Monteiro, F. M., Yool, A., and Ridgwell, A.: EcoGEnIE 1.0: plankton ecology in the cGEnIE Earth system model, Geosci. Model Dev., 11, 4241–4267, https://doi.org/10/gfjrbk, 2018.

Watterson, I. G.: Improved Simulation of Regional Climate by Global Models with Higher Resolution: Skill Scores Correlated with Grid Length*, 28, 5985–6000, https://doi.org/10.1175/JCLI-D-14-00702.1, 2015.

West, G. B., Brown, J. H., and Enquist, B. J.: A General Model for the Origin of Allometric Scaling Laws in Biology, Science, 276, 122–126, https://doi.org/10.1126/science.276.5309.122, 1997.

Zakharova, L., Meyer, K. M., and Seifan, M.: Trait-based modelling in ecology: A review of two decades of research, Ecological Modelling, 407, 108703, https://doi.org/10.1016/j.ecolmodel.2019.05.008, 2019.

Žarić, S., Schulz, M., and Mulitza, S.: Global prediction of planktic foraminiferal fluxes from hydrographic and productivity data, 3, 187–207, https://doi.org/10/ddgc7j, 2006.